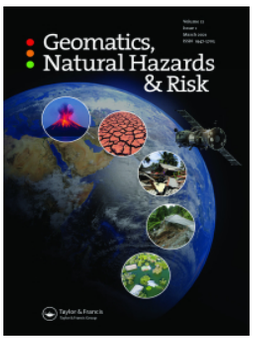

Geomatics, Natural Hazards and Risk

ISSN: (Print) (Online) Journal homepage: https://www.tandfonline.com/loi/tgnh20

Understanding spatiotemporal patterns of typhoon storm surge disasters based on their tropical cyclone track clusters in China

Ke Wang, Yongsheng Yang, Genserik Reniers & Quanyi Huang

To cite this article: Ke Wang, Yongsheng Yang, Genserik Reniers & Quanyi Huang (2021) Understanding spatiotemporal patterns of typhoon storm surge disasters based on their tropical cyclone track clusters in China, Geomatics, Natural Hazards and Risk, 12:1, 2736-2754, DOI: 10.1080/19475705.2021.1973120

To link to this article: https://doi.org/10.1080/19475705.2021.1973120

Published online: 24 Sep 2021.

GEOMATICS, NATURAL HAZARDS AND RISK
2021, VOL. 12, NO. 1, 2736–2754
https://doi.org/10.1080/19475705.2021.1973120

Taylor & Francis
Taylor & Francis Group

Understanding spatiotemporal patterns of typhoon storm surge disasters based on their tropical cyclone track clusters in China

Ke Wang[a,b,c], Yongsheng Yang[a,b], Genserik Reniers[c,d,e] and Quanyi Huang[a,b]

[a]Institute of Public Safety Research, Department of Engineering Physics, Tsinghua University, Beijing, China; [b]Beijing Key Laboratory of City Integrated Emergency Response Science, Tsinghua University, Beijing, China; [c]CEDON, KU Leuven, Brussels, Belgium; [d]Safety and Security Science Group, Faculty of Technology, Policy and Management, TU Delft, Delft, The Netherlands; [e]Faculty of Applied Economics, Antwerp Research Group on Safety and Security (ARGoSS), University of Antwerp, Antwerp, Belgium

ABSTRACT

Typhoon storm surge disasters have garnered much attention because of their catastrophic damages. We investigated spatiotemporal patterns of typhoon storm surge disasters based on their tropical cyclone track clusters to support disaster mitigation in China. We aggregated 172 typhoon storm surge disasters in the entire cluster. Then, we used the extended Finite-Mixture-Model to categorize these 172 disasters into three clusters according to their track clusters (westward, northward, and westward shift at the coastline). In general, not all temporal distributions of the frequency and damage showed significant trends in the entire cluster and three clusters from 1983–2018. Between 1983–2000 and 2001–2018, the average annual frequency increased, and average annual direct economic loss and average annual fatalities decreased in the entire cluster. Although most temporal patterns in the three clusters were similar to those in the entire cluster, a positive growth ratio in the average annual direct economic loss was apparent between 1983–2000 and 2001–2018 in Cluster 3. For spatial patterns, southern and eastern regions were more affected by typhoon storm surge disasters than northern regions. In northern regions, Cluster 2 recorded the most disaster occurrences, direct economic losses, and fatalities. Track characteristics and mitigation measures were introduced to help understand disaster spatiotemporal patterns in the entire cluster and three clusters.

ARTICLE HISTORY
Received 11 January 2021
Accepted 20 August 2021

KEYWORDS
Typhoon storm surge disaster; spatiotemporal patterns; tropical cyclone tracks; track clustering; mitigation measures

1. Introduction

A typhoon storm surge (i.e., tropical storm surge or hurricane surge) is an abnormal rise in the seawater level caused by strong winds and sudden pressure changes

CONTACT Quanyi Huang qyhuang@tsinghua.edu.cn

typically associated with tropical cyclones (Grinsted et al. 2013; Needham et al. 2013). Coupled with an astronomical tide and wave, a typhoon storm surge disaster (TSSD) may occur (State Oceanic Administration of China 2017) and can severely impact (e.g., coastal flooding) coastal areas (Cheung et al. 2003; Rodrigo et al. 2018). According to the Bulletin of China Marine Disaster (1989-2018), TSSDs are the most destructive marine disasters in China, causing losses higher than the total direct economic losses from all other marine disasters. In 2018, direct economic losses from TSSDs accounted for approximately 90% of total marine disaster losses in China. Furthermore, 14 administrative coastal regions at the province level in China have been affected by TSSDs. A sea-level rise (Overpeck et al. 2006; Rahmstorf 2007) and possibly more intense tropical cyclones (Knutson et al. 2010) under climate change are likely to increase the TSSD risk (Dasgupta et al. 2009; Hallegatte et al. 2013; Lloyd et al. 2016). According to the MNRC (2019), China's coastal sea level will rise by 68–166 mm in the next 30 years. Most TSSDs in China have been caused by tropical cyclones generated in the northwest Pacific (Ling et al. 2011). Yasuda et al. (2014) predicted that the intensity of tropical cyclones would likely increase in the northwest Pacific in the future. Additionally, the coastal population and economy are growing (Neumann et al. 2015; Gao and Wang 2020; Winther et al. 2020), making the coastal areas more vulnerable to TSSDs (Helderop and Grubesic 2019). National Bureau of Statistics (2019) reports that the coastal population in mainland China rose by 17% from 2000 to 2018. Hence, a better understanding of TSSD spatiotemporal patterns is vital for disaster mitigation in China.

Previous studies have examined TSSDs' spatiotemporal patterns and related factors in China. Sun et al. (2013) investigated spatiotemporal patterns of TSSDs in Guangxi, a coastal province in China; the present study investigated contributors to them, such as tropical cyclone tracks, harbour terrains, and atmospheric and gulf resonances. Gan et al. (2012) focused on spatiotemporal patterns of TSSDs in three of China's southern coastal regions and highlighted relevant factors, such as tropical cyclone tracks, intensities, typhoon storm surges combining with astronomical high tides, and terrains. Some researchers have analyzed spatiotemporal patterns in 11 coastal regions of mainland China and detailed mitigation measures, while discussion of other related factors has been restricted because of limited data on a large spatial scale for these coastal regions in China (Shi et al. 2015; Fang et al. 2017; Wang, Liu, et at. 2021; Wang, Yang, et al. 2021).

Tropical cyclones are crucial in TSSD generation; they contribute via tracks, intensities, forward speeds, and sizes (Resio and Westerink 2008). Colle et al. (2010) presented two aspects of cyclones concerning storm surge events: (1) evolution of the wind speed and direction around New York City for storm surge events with varying intensities, and (2) types of cyclone positions and tracks favouring storm surge events in the New York City area. A few studies have outlined the relationship between tropical cyclone tracks and storm surge events. Haigh et al. (2016) distinguished storm tracks that generated extreme sea level events around the coastline of the UK. Bromirski et al. (2017) analyzed the intensities and tracks of storms causing surges along the Pacific coast of North America. Du et al. (2020) investigated the impact of three typhoon track types on storm surges in Zhejiang, one coastal region in China.

Such explorations are essential to improving the understanding of spatiotemporal patterns regarding TSSDs. Although some studies depicted TSSD spatiotemporal patterns and classified tracks of tropical cyclones causing these TSSDs in China (e.g., Hou et al. 2011), little attention has been paid to understanding TSSD spatiotemporal patterns based on their tropical cyclone tracks. Tropical cyclone tracks near the coastline are necessary to identify coastal regions that may be affected (Colle et al. 2010; Booth et al. 2016; Bromirski et al. 2017). Consequently, this study extends the literature to explore spatiotemporal patterns of TSSDs based on tropical cyclone track types in China.

Many methods have been introduced to cluster tropical cyclone tracks. Some studies qualitatively classified tropical cyclone tracks (e.g., Meng et al. 2005), while others proposed a quantitative classification of the results of specific parameters. Liu et al. (2018) grouped typhoons making landfall in China into three types utilizing arctangents of zonal and meridional velocities calculated by average post-landfall movement velocities. Numerous studies have clustered tropical cyclone tracks using different algorithms as well. Nakamura et al. (2009) used a two-moment clustering method derived from the K-means method. Others (Elsner 2003; Corporal-Lodangco et al. 2014) conducted clustering by modifying the method of Nakamura et al. (2009). Multiple researchers introduced methods based on fuzzy c-means (Kim et al. 2011) and self-organizing maps (Kim and Seo 2016) to cluster tropical cyclone tracks. However, methods based on K-means, fuzzy c-means, and self-organizing maps employ a fixed number of vector lengths, which may lead to a loss of tempo-spatial information. Tracks of various lengths are accommodated by an extension of the Finite-Mixture-Model (FMM), which uses regression mixture models to cluster tracks (Gaffney and Smyth 1999; Gaffney et al. 2007). Some researchers have also conducted tropical track clustering in the Western North Pacific Ocean and the Western Indian Ocean via this extended FMM (Camargo et al. 2007a, 2007b; Ramsay et al. 2012; Grinsted et al. 2013; Geng et al. 2016). Since tropical cyclone tracks inducing TSSDs were usually of different lengths, we preferred the extended FMM to cluster the surge-producing tropical cyclone tracks in China.

Although many factors of tropical cyclones can contribute to TSSDs, this study focused on exploring spatiotemporal patterns of TSSDs from the perspective of the tropical cyclone track. The main contribution of this study is that it assigned TSSDs into different clusters according to their surge-producing tropical cyclone tracks using the extended FMM, and it explored spatiotemporal patterns of TSSDs in the entire cluster (EC) and separate clusters. The remainder of this paper is organized as follows: Section 2 defines the materials and methods used, and Section 3 reveals spatiotemporal patterns of TSSDs in the EC and different clusters. Sections 4 and 5 present the discussion and conclusions, respectively.

2. Materials and methods

In this section, we introduce the study area and describe the data collection. Subsequently, the extended FMM is explained and employed to cluster surge-producing tropical cyclone tracks. The corresponding TSSDs are assigned to different

Figure 1. The 11 coastal regions as the study area.

clusters according to the cluster result of their surge-producing tropical cyclone tracks. Finally, we present the calculation equations used in this study.

2.1. Study area and data collection

Although TSSDs impacted 14 coastal regions at the province level in China, 11 of them (Figure 1) were selected as the study area because no disaster data were available for Hong Kong, Macao, or Taiwan from our data sources. In 2018, both the population and gross regional product in the chosen regions account for approximately 50% of the total values in mainland China, according to the National Bureau of Statistics (2019). As illustrated in Figure 1, these regions were specified as southern (Hainan, Guangxi, and Guangdong), eastern (Fujian, Zhejiang, Shanghai, and Jiangsu), and northern regions (Shandong, Hebei, Tianjin, and Liaoning) to interpret spatial patterns easily.

This study collected data regarding TSSDs, surge-producing tropical cyclone tracks, and economic data. To explore temporal (interannual and monthly) and spatial patterns of the frequency and damage (i.e., the direct economic loss and number of fatalities), the collected TSSD data included disaster ID number, disaster occurrence time (years and months), total damages, affected coastal regions, and damages in the

individual coastal region. Data were gathered from three sources, namely the Bulletin of China Marine Disaster (State Oceanic Administration of China 1989–2018), Collection of Storm Surge Disaster Historical Data in China 1949-2009 (Yu et al. 2015), and the Bulletin of Guangxi Marine Ecological Environment Status (Oceanic Administration of Guangxi 2008–2009). During the TSSD data collection, we followed two rules to obtain accurate and consistent data from the three data sources. The first rule was that if one TSSD was reported by more than one data source, data from the Bulletin of China Marine Disaster were used. The second rule was that if the damage data from one TSSD were insufficient in one data source, the consistency of the total damage data had to be affirmed before supplementing the damage data from other sources. Details concerning 172 TSSDs occurring between 1983–2018 were thus collected for this study. Then, we collected surge-producing tropical cyclone tracks of these 172 TSSDs from the Best Track Database (Ying et al. 2014; Lu et al. 2021), which is publicly accessible (STI 2020). Data of tracks included their ID numbers and track points (latitudes and longitudes). The disaster ID number of a TSSD is the same as the ID number of its surge-producing tropical cyclone. For example, the "1409" tropical cyclone caused the "1409" typhoon storm surge disaster. Finally, we obtained the Consumer Price Index (CPI) for 1983–2018 from the China Economic and Social Big Data Research Platform (CESD 2020) to normalize direct economic losses from TSSDs.

2.2. Analysis methods

For the standard FMM framework, the probability density function (PDF) is given by (Gaffney et al. 2007)

$$p(\boldsymbol{x} \mid \emptyset) = \sum_{k}^{K} \alpha_k p_k(\boldsymbol{x} \mid \theta_k) \tag{1}$$

in which $\boldsymbol{x}$ is a d-dimensional vector, α_k is the nonnegative weight for the *kth* component and the sum of α_k is one, p_k is the density of the *kth* component regarding the parameter θ_k.

The description for the data clustering through the FMM is as follows (Gaffney et al. 2007). For an observed data set $\boldsymbol{x} = \{x_1, x_2, \ldots, x_n\}$, each vector x_i is generated by one of the K clusters. The Expectation-Maximization algorithm can be used to estimate parameters for the PDF. Given the probability that the *kth* cluster generated $\boldsymbol{x}$ can be calculated by the Bayes rule based on the estimated parameters, $\boldsymbol{x}$ can be assigned to the cluster that has the highest posterior probability. Gaffney (2004b) developed regression mixture models based on the FMM to cluster tracks. In this extended FMM framework, each track ($\boldsymbol{x}$) is a multiple-order polynomial regression function for modelling the track's latitudinal and longitudinal positions versus time (Camargo et al. 2007a); the track can be clustered according to FMM procedures. Gaffney (2004a) generated the clustering algorithms of the extended FMM into a MATLAB toolbox, called the curve clustering toolbox (CCToolbox)—the specifications of clustering algorithms refer to Gaffney (2004b).

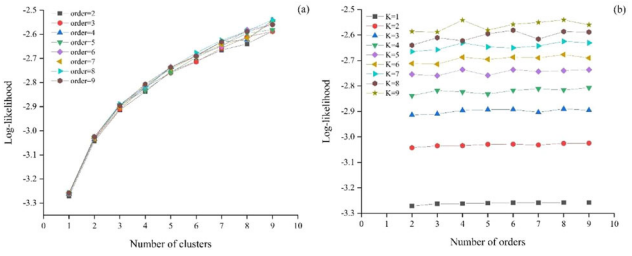

Figure 2. Log-likelihood scores for (a) clusters and (b) orders.

We employed the CCToolbox to cluster 172 tropical cyclone tracks, and we used the criterion of cross-validated log-likelihood scores in the study of Huang (2018) to choose the order of the polynomial regression function and the number of clusters (K). We tested 72 combinations for orders and Ks, and the findings are displayed in Figure 2. As evident from Figure 2(a), most log-likelihood values increased as the number of orders and clusters increased, but returns of improvement diminished beyond order = 5, indicating that the possible orders were between three and five. For K = 3, the log-likelihood values increased and did not fluctuate until the number of orders was six (Figure 2b). Likewise, for K = 4 and K = 5, fluctuations occurred after order = 2 and order = 3 (Figure 2b). Subsequently, the order and K can be chosen from three combinations: order = 6 and K = 3; order = 2 and K = 4; and order = 3 and K = 5.

The average annual number of TSSDs in each cluster should be more than one to show the TSSD frequency over time. According to Table 1, only one combination, order = 6 and K = 3, was qualified. Hence, we categorized 172 tropical cyclone tracks into three clusters. Correspondingly, all 172 TSSDs were aggregated in the EC, and these TSSDs were assigned to the corresponding cluster according to the cluster result of their surge-producing tropical cyclone tracks. The EC and the three clusters included data of TSSDs and tracks of tropical cyclones with corresponding ID numbers. Based on TSSDs in different clusters, we explored their spatiotemporal patterns.

The collected damage data included direct economic loss and fatality records. We used the inflation ratio (i.e., CPI) to normalize direct economic losses into values in 2018, which is the same normalization method used in a study showing the direct economic loss trend of TSSDs during 1983–2018 in China (Wang, Yang, et al. 2021).

In this study, we analyzed the temporal patterns of the frequency and damage using the average annual value before and after 2000. The reason we divided our study period is explained in Section 3.2. The average annual value (AAV) was calculated by the total value (TV) and the number of years (N), as given by

$$AVV_{1983\text{–}2000} = \frac{TV_{1983\text{–}2000}}{N_{1983\text{–}2000}} \tag{2}$$

$$AVV_{2001\text{–}2018} = \frac{TV_{2001\text{–}2018}}{N_{2001\text{–}2018}} \tag{3}$$

Table 1. The number of typhoons in each cluster regarding different numbers of clusters.

The K and the order	The number of tropical cyclones in each cluster	The average number of typhoons per year in each cluster (1983–2018)
K = 3 and order = 6	Cluster 1: 74	Cluster 1: 2.06
	Cluster 2: 54	Cluster 2: 1.50
	Cluster 3: 44	Cluster 3: 1.22
K = 4 and order = 2	Cluster 4–1: 52	Cluster 4–1: 1.44
	Cluster 4–2: 30	Cluster 4–2: 0.83
	Cluster 4–3: 35	Cluster 4–3: 0.97
	Cluster 4–4: 55	Cluster 4–4: 1.53
K = 5 and order = 3	Cluster 5–1: 32	Cluster 5–1: 0.89
	Cluster 5–2: 33	Cluster 5–2: 0.92
	Cluster 5–3: 42	Cluster 5–3: 1.17
	Cluster 5–4: 29	Cluster 5–4: 0.81
	Cluster 5–5: 36	Cluster 5–5: 1.00

The growth ratio of the average annual value (GR) between 1983–2000 and 2001–2018 was given by

$$GR = \frac{AVV_{2001-2018} - AVV_{1983-2000}}{AVV_{1983-2000}} \tag{4}$$

3. Results

3.1. Clustering results

We aggregated 172 TSSDs in the EC. As demonstrated in Section 2.2, 172 tracks of tropical cyclones (Figure 3a) in the EC were clustered into three clusters through the CCToolbox (Figure 3). Cluster 1 (C1) constituted 74 tracks (Figure 3b), and most of the tracks moved westward towards the coastal regions. For the 54 tracks in Cluster 2 (C2), nearly all had a northward shift along the coastline (Figure 3c). Altogether, 44 tracks in Cluster 3 (C3) had a westward shift similar to C1, but genesis positions in C1 and C3 showed apparent differences (Figure 3b and d). These three track categories were consistent with the clustering results of Geng et al. (2016), in which landfall tropical cyclone tracks from 1951–2012 in China were clustered into three clusters via the CCToolbox. Notably, segments of tropical cyclones near the coastline are primarily responsible for TSSDs, especially landfall sites (Bromirski et al. 2017). Tropical cyclone track segments alongside the coastline are influenced by many factors, including genesis locations (Colbert et al. 2015) and previous movement patterns (Dvorak 1975; Kovordányi and Roy 2009; Roy and Kovordányi 2012). Therefore, we categorized whole tracks into clusters instead of utilizing track segments near the coastline to analyze the spatiotemporal patterns of TSSDs. Also, some studies exploring TSSD spatiotemporal patterns have used the whole track categorization to investigate track types (Hou et al. 2011; Gan et al. 2012; Sun et al. 2013; Wang et al. 2014). Based on the tropical cyclone track cluster result, the corresponding TSSD was assigned to each cluster. Spatiotemporal patterns of TSSDs in the EC and each cluster are explored as follows.

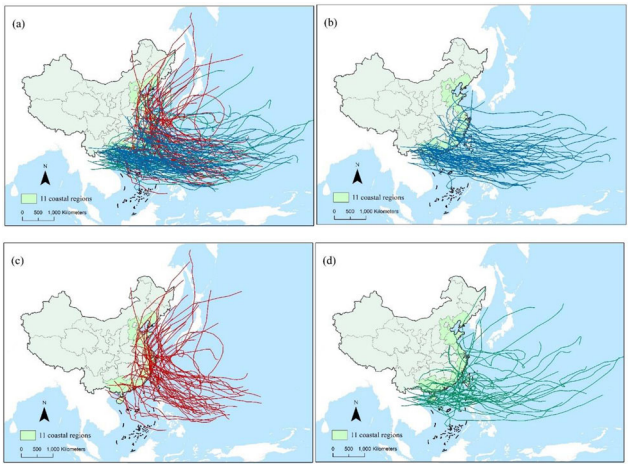

Figure 3. Tropical cyclone tracks in the (a) EC, (b) C1, (c) C2, and (d) C3.

3.2. Temporal patterns of TSSDs

In the EC, C1, and C2, an increasing trend in the annual frequency was witnessed between 1983 and 2018 (Figure 4). However, there was no significant trend in the TSSD frequency (at 0.05 significance) in C3 during 1983–2018. As Fang et al. (2017) noted, there has been an increase in the frequency of storm surge disasters since 2000. In this study, we used the year 2000 to divide the study period to further analyze the growth ratio of the average annual frequency (AAF) before and after 2000 in the EC and three clusters (Table 2).

In Table 2, the AAF in the EC after 2000 (6.4) was more than twice before 2000 (3.1). Similarly, the AAFs in all three clusters increased after 2000 (Table 2). In Table 2, we can see that growth ratios in C1 (115%) and C2 (175%) were greater than those in the EC (106%), and the growth ratio in C3 was the lowest (40%). The years reporting the highest annual frequency (Table 2) are those after 2000 as well. However, there is an inconsistency in years with the highest annual frequency between the EC (in 2013) and the three clusters.

The monthly distribution of the TSSD frequency is shown in Figure 5, and all collected TSSDs in the EC were recorded from April to November. The number of TSSD occurrences between July and September accounted for about 80% (Table 3) of the total numbers in 12 months in the EC and three clusters. Although August revealed a peak occurrence of TSSDs in EC, C1, and C2, September denoted the highest number of TSSDs in C3. In C2, the earliest TSSD was in April, which was also the earliest occurrence month record among all 172 TSSDs. Conversely, the latest month of occurrence in a given year was November in C3.

Annual direct economic losses from TSSDs are displayed in Figure 6a. There were no significant trends (at 0.05 significance) in direct economic losses from 1983 to 2018 in the EC and three clusters. A decrease in direct economic losses after 2000 compared to before 2000 was observed in the EC, C1, and C2, while the opposite pattern was found in C3 (Table 4). In the EC, the average annual direct economic loss (ADCL) after 2000 (134) was lower than before (178). Table 4 also shows a decrease

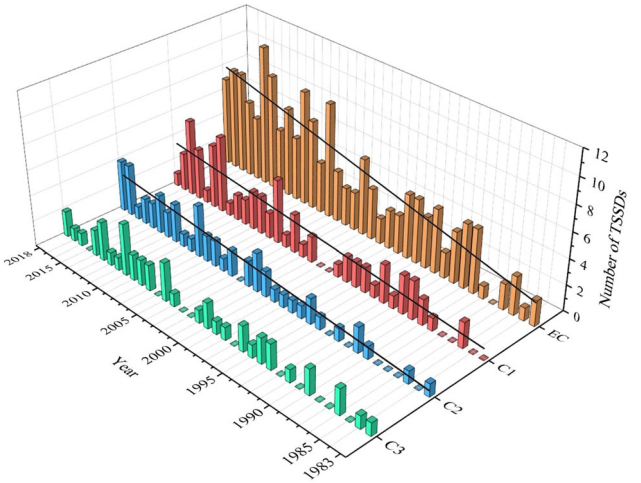

Figure 4. Number of TSSDs per year in the EC, C1, C2, and C3 (black lines indicate linear trends at 0.05 significance).

Table 2. AAFs and years with the highest annual frequency in the EC and three clusters.

Cluster	AAF during 1983–2000	AAF during 2001–2018	The Growth Ratio of AAFbetween 1983–2000 and 2001–2018	Years with the Highest Annual Frequency
EC	3.1	6.4	106%	2013 (11)
C1	1.3	2.8	115%	2016 (6)
				2012 (6)
C2	0.8	2.2	175%	2018 (4)
				2017 (4)
				2008 (4)
C3	1.0	1.4	40%	2010 (4)

in the ADCL before and after 2000 in C1 (-32%) and C2 (-42%). However, the positive growth ratio in C3 was notable at 24%. In C3, two years (2005 and 2008) with the highest direct economic losses were observed after 2000, while the two years with the highest direct economic losses in the EC, C1, and C2 were before 2000 (Table 4).

Figure 6b shows a significantly decreasing trend in the number of fatalities in the EC from 1983 to 2018. Although similar decreasing trends were not observed (at 0.05 significance) in all three clusters, a relatively significant decline in average annual fatalities (AFs) after 2000 was observed in Table 4. In Table 4, we can see that AFs in C1 in the second period (2001–2018) decreased sharply (-93% growth ratio) compared with the first period (1983–2018). The year with the highest fatalities (Table 4) was 1994 for EC and C1, 2006 for C2, and 1986 for C3; the highest annual fatality record in C1 (1216 fatalities) was far greater than that in C2 (326 fatalities) and C3 (211 fatalities).

3.3. Spatial patterns of TSSDs

Generally, southern and eastern regions sustained more damages than northern regions in the EC and three clusters. The percentage of damages in four northern regions in C2 was far greater than C1 and C3.

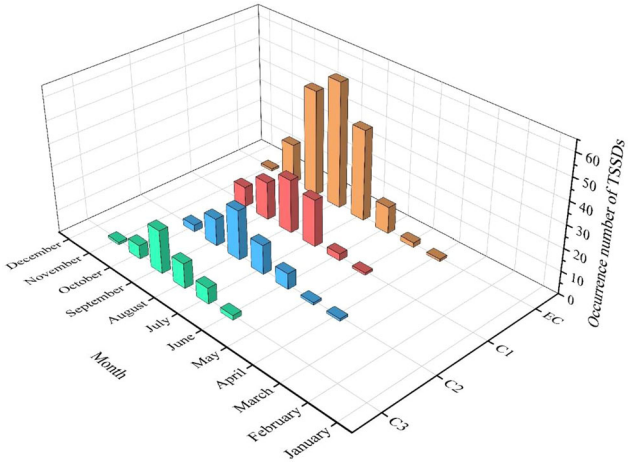

Figure 5. Occurrence number of TSSDs per month in the EC, C1, C2, and C3.

Table 3. Some temporal patterns in the number of TSSDs per month.

Cluster	The Ratio of the Occurrence Number of TSSDs between July and September to the Total Number of TSSDs in 12 Months	Three Months with the Highest TSSD Occurrence Record in a Descending Order	Months with the Earliest TSSD Record	Months with the Furthest TSSD Record
EC	81%	August September July	April	November
C1	83%	August July September	May	October
C2	80%	August July September	April	October
C3	80%	September August July	June	November

In Figure 7(a–d) and Table 5, the spatial patterns in the EC and all three clusters show that the southern and eastern regions experienced more TSSD occurrences than the northern regions. In the EC (Figure 7a and Table 5), the three regions with the highest TSSD occurrences included a southern region (Guangdong) and two eastern regions (Fujian and Zhejiang). TSSD occurrences in the four northern regions (Shandong, Hebei, Tianjin, and Liaoning) represented only 9% (30) of all occurrences in the 11 coastal regions (324 occurrences). The three places with the highest TSSD occurrences in the three clusters were in the southern and eastern coastal regions (Figure 7b–d and Table 5). However, among the three clusters, differences in TSSD occurrences in the four northern regions were quite significant. In C1 and C3 (Figure 7b and d), TSSD occurrences in the four northern regions both accounted for less than 5% (6 and 3 occurrences, respectively) of the total occurrences in the 11 coastal regions (133 and 79 occurrences, respectively). However, this percentage was more than 18% (21 occurrences) in C2 (112 occurrences), as seen in Figure 7c, validating

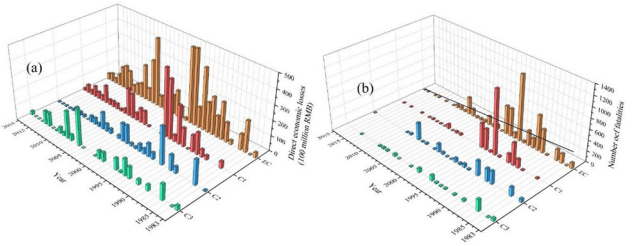

Figure 6. (a) Direct economic losses of TSSDs per year in the EC, C1, C2, and C3; (b) the number of fatalities of TSSDs per year in the EC, C1, C2, and C3 (the black line indicates the linear trend at 0.05 significance).

Table 4. Some temporal patterns in damages from TSSDs per year.

Cluster	EC	C1	C2	C3
ADCL (100 million RMB) during 1983–2000	178	93	52	33
ADCL (100 million RMB) during 2001–2018	134	63	30	41
The Growth Ratio of ADCL between 1983–2000 and 2001–2018	−25%	−32%	−42%	24%
Three Years with Highest	1996	1997	1992	2005
Annual Direct Economic	1997	1996	1985	2008
Losses in a Descending Order	2005	1994	2000	1994
AFs during 1983–2000	257	162	67	29
AFs during 2001–2018	50	11	31	7
The Growth Ratio of AFs between 1983–2000 and 2001–2018	−81%	−93%	−54%	−76%
The Year with the Highest Annual Fatalities	1994 (1240)	1994 (1216)	2006 (326)	1986 (211)

that 70% of the total TSSD occurrences in the four northern regions were noted in C2.

The spatial distribution of direct economic losses from TSSDs is outlined in Figure 7(e–h). In the EC and all three clusters, direct economic losses in the southern and eastern regions were far greater than in the four northern regions, where Shandong and Liaoning reported more direct economic losses than Hebei and Tianjin (Table 5). Besides, direct economic losses in Guangdong, Fujian, and Zhejiang accounted for approximately 78% (435.2 billion RMB) of the total losses (561 billion RMB) in the EC (Figure 7e). However, direct economic losses in the four northern regions accounted for only 8% (47.3 billion RMB) of the total in the EC. Three places with the highest direct economic losses in the three clusters were reported in southern and eastern regions (Figure 7f–h and Table 5), similar to spatial patterns in the EC. Despite four places in the northern region accounting for 8% of the total losses in the EC, the percentage in C2 (148 billion RMB) reached nearly 21% (30.3 billion RMB) and was slightly over 3% (9.7 billion RMB) and 5% (7.2 billion RMB) in C1 (279.8 billion RMB) and C3 (133.2 billion RMB), respectively. Moreover, direct economic losses in the northern regions of C2 represented nearly 65% of the total direct economic losses in the four northern regions.

Figure 7(i–l) exemplifies the spatial patterns of the number of fatalities from TSSDs. Most fatalities were recorded in the southern and eastern regions of the EC and three clusters. The number of fatalities in Zhejiang, Guangdong, and Fujian

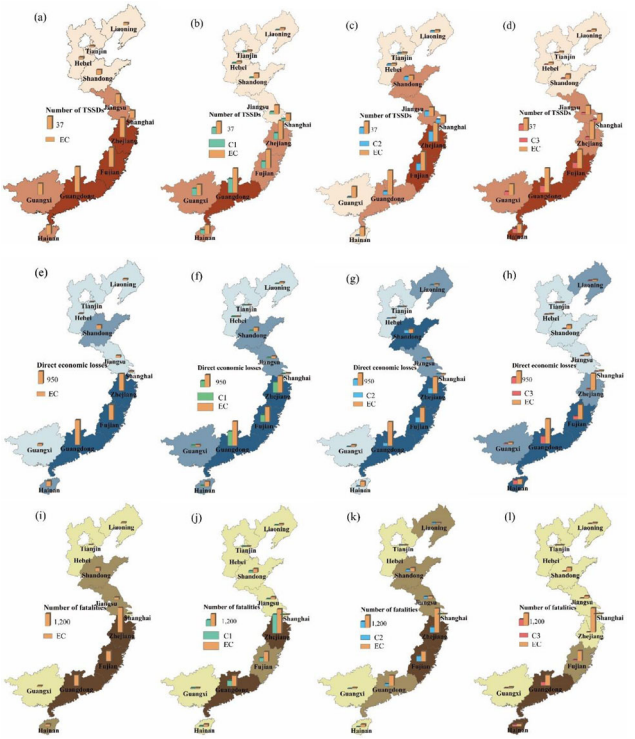

Figure 7. TSSD occurrences per coastal region during 1983-2018 in the (a) EC, (b) C1, (c) C2, and (d) C3; direct economic losses (100 million RMB) from TSSDs per coastal region during 1983-2018 in the (e) EC, (f) C1, (g) C2, and (h) C3; fatalities from TSSDs per coastal region during 1983-2018 in the (i) EC, (j) C1, (k) C2, and (l) C3. Note: colours from dark to light indicate representative numbers from large to small in each figure.

accounted for more than 80% (4452) of the total number of fatalities (5528) in the EC, whereas the number of fatalities in the four northern regions accounted for only 9% (486). In the three clusters, the number of fatalities in the southern and eastern regions was over 80% of the total number of fatalities. The number of fatalities in C2 in the four northern regions accounted for nearly 65% (312) of the total fatalities in the four northern regions of the EC. Additionally, the number of fatalities in four northern regions equaled nearly 18% of the total number of fatalities in C2 (1759), far more than those in C1 (5%) and C3 (2%).

4. Discussion

During 1983–2018, spatiotemporal distributions of TSSDs in the EC were consistent with the TSSD distribution of Wang, Yang, et al. 2021. However, distributions in the three clusters were not completely consistent with those in the EC, highlighting specific patterns in different clusters.

The monthly frequency patterns of TSSDs in different clusters were interesting. In C2, the earliest TSSD record (disaster ID number: 0801) during 1983–2018 was reported in April. The “0801” surge-producing track had a northeastward direction

Table 5. TSSD occurrences and damages of 11 coastal regions in descending order.

Cluster	TSSD Occurrences in 11 Coastal Regions (Descending Order)		Direct Economic Losses in 11 Coastal Regions (Descending Order)		Number of fatalities in 11 Coastal Regions (Descending Order)	
EC	1 Guangdong	2 Fujian	1 Guangdong	2 Zhejiang	1 Zhejiang	2 Guangdong
	3 Zhejiang	4 Guangxi	3 Fujian	4 Hainan	3 Fujian	4 Shandong
	5 Jiangsu	6 Hainan	5 Shandong	6 Jiangsu	5 Hainan	6 Jiangsu
	7 Shanghai	8 Shandong	7 Guangxi	8 Liaoning	7 Liaoning	8 Guangxi
	9 Liaoning	10 Hebei	9 Shanghai	10 Hebei	9 Shanghai	10 Tianjin
	11 Tianjin		11 Tianjin		11 Hebei	
C1	1 Guangdong	2 Guangxi	1 Guangdong	2 Zhejiang	1 Zhejiang	2 Guangdong
	3 Fujian	4 Zhejiang	3 Fujian	4 Guangxi	3 Fujian	4 Shandong
	5 Hainan	6 Jiangsu	5 Hainan	6 Shandong	5 Guangxi	6 Hainan
	7 Shanghai	8 Hebei	7 Jiangsu	8 Hebei	7 Jiangsu	8 Shanghai
	9 Shandong	10 Liaoning	9 Shanghai	10 Liaoning	9 Liaoning	10 Tianjin
	11 Tianjin		11 Tianjin		11 Hebei	
C2	1 Zhejiang	2 Fujian	1 Zhejiang	2 Fujian	1 Zhejiang	2 Fujian
	3 Jiangsu	4 Shanghai	3 Guangdong	4 Shandong	3 Shandong	4 Guangdong
	5 Guangdong	6 Shandong	5 Jiangsu	6 Shanghai	5 Jiangsu	6 Liaoning
	7 Liaoning	8 Hebei	7 Liaoning	8 Tianjin	7 Shanghai	8 Tianjin
	9 Tianjin	10 Guangxi	9 Hebei	10 Hainan	9 Hebei	10 Guangxi
	11 Hainan		11 Guangxi		11 Hainan	
C3	1 Guangdong	2 Fujian	1 Guangdong	2 Hainan	1 Guangdong	2 Hainan
	3 Hainan	4 Guangxi	3 Fujian	4 Zhejiang	3 Fujian	4 Shandong
	5 Zhejiang	6 Jiangsu	5 Liaoning	6 Guangxi	5 Guangxi	6 Jiangsu
	7 Shanghai	8 Shandong	7 Shandong	8 Shanghai	7 Zhejiang	8 Shanghai
	9 Liaoning	10 Tianjin	9 Jiangsu	10 Tianjin	9 Liaoning	10 Tianjin
	11 Hebei		11 Hebei		11 Hebei	

from Hainan to Guangdong, ultimately disappearing in Guangdong. In C3, the furthest record (disaster ID number: 1330) during 1983–2018 was observed in November, and damages were reported in Guangxi. The distressed places highlighted in these two records were all in the southern region, suggesting that southern governments should be active in protecting coastal areas against TSSDs.

ADCL during 2001–2018 was lower than that during 1983–2000 in C1 and C2, respectively, while the opposite pattern was observed in C3 (Table 4). We further analyzed the characteristics of TSSDs in C3 and found severe disasters in 2005, 2008, 2013, and 2014, leading to high direct economic losses in these years. Table 6 elucidates severe TSSDs in these four years, revealing that almost all those affected were situated in the southern regions. Hence, the southern regions should pay particular attention to tropical cyclone tracks in C3, as they may trigger severe TSSDs.

From 1983 to 2018, the fatality trend in the EC indicated a decrease, but no significant decreasing trends were found in all three clusters. However, the significant negative growth ratios of AFs between 1983–2000 and 2001–2018 were observed in the EC and all three clusters (Table 4). Many studies have explicated the mitigation measures adopted in China to discern the decline in damages after 2000 (Shi et al. 2015; Fang et al. 2017; Wang, Liu, et at. 2021; Wang, Yang, et al. 2021). The primary mitigation measures are as follows. (1) Coastal governments have built many new seawalls with high protection standards and reinforced the weaker sections of the old seawalls (Luo et al. 2015). According to Ma et al. (2014), the ratio of seawall length to mainland coastline length has reached approximately 60%. (2) Plantation of mangroves has been encouraged in coastal regions to reduce storm surge water levels, wave energy, and resist seawall erosion (Mcivor et al. 2012; Fan et al. 2013; Spalding

Table 6. Severe TSSDs in C3 during 2005, 2008, 2013, and 2014.

Year	Disaster ID Number	Direct Economic Loss (100 million RMB, 2018 values)	Maximum Surge (cm) / Observation Station	Most Affected Regions according to Direct Economic Losses (Descending Order)
2005	0518	170.19	197 / Nandu	Hainan, Guandong, Guangxi
2008	0814	165.33	270 / Beijin	Guangdong, Guangxi, Hainan
2013	1319	71.06	201 / Haimen	Guangdong, Fujian
2014	1409	86.69	392 / Nandu	Guangdong, Guangxi, Hainan

et al. 2014). (3) The capacity of systems to observe, forecast, and warn about TSSDs has been improved, and the warning information can be disseminated to the public in many ways (China Ocean Yearbook Compilation Committee 1987–2017). (4) Relevant guidelines have been released to manage TSSDs, such as "Technical Guidelines for Risk Assessment and Zoning of Storm Surge Disasters" and "Specification for Warning Water Level Determination (GB/T 17839–2011)." Such documents can identify TSSD risk levels, supporting scientific spatial planning and emergency plans in different coastal areas. The "Storm Surge Disaster Emergency Response Plan" specifies standardized response procedures to enhance response efficiency. Furthermore, a marine disaster risk census to better manage disasters has been administered. (5) Many activities (e.g., emergency drills) have been executed to raise public awareness. More rescue teams and marine emergency shelters can bolster performance in response to TSSDs (Lixin et al. 2012).

The comprehensive demonstration community of marine disaster reduction has developed an effective management system, including the measures mentioned above, to significantly mitigate the impacts of such disasters (Zhang et al. 2013). The Lianjiang (county) demonstration community, a pioneer, has been established with progressive disaster management policies. Some prevention and mitigation measures have been taken (Zeng 2018; Chen et al. 2019). In 2009, six observation stations were involved in verifying the warning water level in Lianjiang. In 2011, the State Oceanic Administration of China made a TSSD risk assessment, including a hazard assessment of the typhoon storm surge, a vulnerability assessment of Lianjiang, an assessment of potentially inundated areas, and a determination of evacuation routes. The signs of the warning water level and disaster assessment results have been instituted to remind people about the danger of TSSDs, and guide signs for shelters have been installed to help people evacuate to safe places. The observation system and the disaster information release system ensure real-time monitoring and early warning release. Regular response training for all participants (e.g., government managers, residents, and rescue teams) under simulating TSSD scenarios can enhance the capacity of the whole community against disasters. The Lianjiang demonstration community ensures a seamless disaster information transfer at the county, township, and village levels. The standardization workflow of the Lianjiang demonstration community can provide TSSD management experiences for other coastal areas.

The southern and eastern regions were more affected than the northern regions in the EC and all three clusters. More tropical cyclone tracks were near the coastline of the southern and eastern regions, which may contribute to higher TSSD occurrences. In the northern regions, 70% of the total TSSD occurrences were reported in C2. From the perspective of tracks, those near the coastline in C2 mostly moved

Table 7. The differences concerning the spatial affected region scale in three clusters.

Cluster	Average Number of Coastal Regions Affected by Each TSSD	Percentage of TSSDs Affecting More than Two Coastal Regions	Number of TSSDs affecting Northern Regions
C1	1.8	18%	2
C2	2.07	26%	12
C3	1.8	23%	2

northward, affecting the northern regions (Figure 3c). Also, tracks in C2 near the coastline spanned more coastal regions than those in C1 and C2, leading to more affected regions of a single disaster in C2 (Table 7). For instance, one TSSD (disaster ID: 9216) with the largest affected spatial scale struck seven coastal regions—Fujian, Zhejiang, Jiangsu, Shandong, Tianjin, Hebei, and Liaoning.

Similar to the spatial frequency distributions in the EC and three clusters, most damages were observed in southern and eastern regions. More tropical cyclone tracks near the coastline of the southern and eastern regions can harm these regions. In C2, most tracks with a northward shift may be the factor causing more destruction in northern regions than in southern and eastern regions.

5. Conclusions

In this study, we collected 172 TSSDs from 1983–2018 in 11 coastal regions of China, and these TSSDs were aggregated in the EC. We clustered surge-producing tropical cyclones of 172 TSSDs into three clusters, and then assigned 172 TSSDs to three clusters according to their tracks. We explored spatiotemporal patterns of the frequency and damage of TSSDs in the EC and three clusters. Although we discovered many similarities in the spatiotemporal distributions, we also observed some inconsistencies in the spatiotemporal distributions between the EC and three clusters. Compared with spatiotemporal distributions in the three clusters, more valuable findings were presented: (1) Among the three clusters, C1 contained the highest number of TSSDs. (2) Between 1983–2000 and 2001–2018, there was an increase in the AAF and a decrease in the ADCL and AFs in C1 and C2. In C3, similar growth ratios of the AAF and AFs were observed during the same two periods, but a significant difference (a positive growth ratio) was noticed regarding the ADCL. After 2000, almost all the affected regions from severe TSSDs in C3 were located in the southern regions, implying that these regions should prepare for possibly severe TSSDs in the future. (3) Most TSSD occurrences were recorded between June and October in all three clusters. August saw TSSD occurrence peaks between 1983 and 2018 in C1 and C2, while September reported a peak in C3 during the same period. Furthermore, C3 recorded the latest TSSD occurrence month (November) in one southern region among 172 TSSDs, and C2 recorded the earliest TSSD occurrence month (April) in two southern regions among 172 TSSDs. These results emphasize that all coastal governments should protect people and assets against TSSDs from June to October, while southern region governments should be concerned about potential TSSDs in other months (e.g., April). (4) More TSSD occurrences and damages were witnessed in southern and eastern regions in all three clusters from 1983 to 2018. (5) For TSSD occurrences and damages in the four northern regions between 1983 and 2018, 70%

of TSSD occurrences and nearly 65% of damages were recorded in C2. Before TSSDs strike, southern and eastern governments should observe all track types that may generate TSSDs, while northern governments should carefully monitor the northward shift tracks in C2. This study also used track characteristics and introduced mitigation measures to help understand the spatiotemporal distributions in the EC and three clusters. These outcomes support the scientific and effective management of TSSDs for different regional governments to reduce damages.

TSSDs are complex phenomena that comprise many factors, such as related hazards (tropical cyclones, tides, and waves), vulnerability and mitigation measures of coastal regions, and climate change. One limitation of this study is that it only explored the spatiotemporal patterns of TSSDs based on different surge-producing tropical cyclone track clusters. From the perspective of related factors included in surge-producing tropical cyclones, other related factors, such as the intensity, forward speed, size, and landfall site, should be investigated to understand TSSD spatiotemporal patterns in future work.

Disclosure statement

No potential conflict of interest was reported by the authors.

Funding

This work was supported by the National Key Research and Development Plan of China (Grant Number 2017YFC1405301).

References

Booth JF, Rieder HE, Kushnir Y. 2016. Comparing hurricane and extratropical storm surge for the Mid-Atlantic and Northeast Coast of the United States for 1979–2013. Environ Res Lett. 11(9):094004.

Bromirski PD, Flick RE, Miller AJ. 2017. Storm surge along the Pacific coast of North America. J Geophys Res Oceans. 122(1):441–457.

Camargo SJ, Robertson AW, Gaffney SJ, Smyth P, Ghil M. 2007a. Cluster analysis of typhoon tracks. part I: General properties. J Climate. 20(14):3635–3653.

Camargo SJ, Robertson AW, Gaffney SJ, Smyth P, Ghil M. 2007b. Cluster analysis of typhoon tracks. Part II: large-scale circulation and ENSO. J Climate. 20(14):3654–3676.

CESD (China Economic and Social Big Data Research Platform). 2020. Vulnerability and mitigation attribute data. [accessed 2020 Jul 15]. http://data.cnki.net/YearData/Analysis.

Chen XP, Zeng YD, Li XD, Chen JR, Zheng XJ, Li X. 2019. Emergency management system of marine hazards: a case study of the Lianjiang comprehensive demonstration zone against marine disasters. Ocean Dev Manag. 39(03):38–44. (Chinese).

Cheung KF, Phadke AC, Wei Y, Rojas R, Douyere YJ-M, Martino CD, Houston SH, Liu PL-F, Lynett PJ, Dodd N, et al. 2003. Modeling of storm-induced coastal flooding for emergency management. Ocean Eng. 30(11):1353–1386.

China Ocean Yearbook Compilation Committee 1987–2017. China ocean yearbook. Beijing: China Ocean Press.

Colbert AJ, Soden BJ, Kirtman BP. 2015. The impact of natural and anthropogenic climate change on western north Pacific tropical cyclone tracks. J Climate. 28(5):1806–1823.

Colle BA, Rojowsky K, Buonaito F. 2010. New York city storm surges: climatology and an analysis of the wind and cyclone evolution. J Appl Meteorol Climatol. 49(1):85–100.
Corporal-Lodangco IL, Richman MB, Leslie LM, Lamb PJ. 2014. Cluster analysis of north Atlantic tropical cyclones. Procedia Comput Sci. 36:293–300.
Dasgupta S, Laplante B, Murray S, Wheeler D. 2009. Climate change and the future impacts of storm-surge disasters in developing countries. Center for Global Development. https://papers.ssrn.com/abstract=1479650.
Du M, Hou Y, Qi P, Wang K. 2020. The impact of different historical typhoon tracks on storm surge: A case study of Zhejiang, China. J Mar Syst. 206:103318.
Dvorak VF. 1975. Tropical Cyclone Intensity Analysis and Forecasting from Satellite Imagery. Mon Wea Rev. 103(5):420–430.
Elsner JB. 2003. Tracking hurricanes. Bull Amer Meteor Soc. 84(3):353–356.
Fan H, He B, Pernetta JC. 2013. Mangrove ecofarming in Guangxi Province China: an innovative approach to sustainable mangrove use. Ocean Coast Manag. 85:201–208.
Fang J, Hinkel J, Shi P, Nicholls RJ, Saini Y, Brown S, Liu W, Shi X. 2017. Spatial-temporal changes of coastal and marine disasters risks and impacts in Mainland China. Ocean Coastal Manag. 139:125–140.
Gaffney SJ, Robertson AW, Smyth P, Camargo SJ, Ghil M. 2007. Probabilistic clustering of extratropical cyclones using regression mixture models. Clim Dyn. 29(4):423–440.
Gaffney S, Smyth P. 1999. Trajectory clustering with mixtures of regression models. In: Proceedings of the Fifth ACM SIGKDD International Conference on Knowledge Discovery and Data Mining. [Place Unknown]; p. 63–72.
Gaffney S. 2004a. The curve clustering toolbox.. [accessed 2020 Apr 5]. http://www.datalab.uci.edu/resources/CCT/.
Gaffney S. 2004b. Probabilistic curve-aligned clustering and prediction with regression mixture models [dissertation]. Irvine: University of California, Irvine.
Gan SD, Zhang WS, Zong HC, Zhang JS, Lin RD. 2012. Analysis of typhoon storm surge disasters along the south China coast and disaster prevention measures. Hydro-Sci Eng. (6):51–58. (Chinese). doi: 10.16198/j.cnki.1009-640x.2012.06.001
Gao X, Wang X. 2020. The trends of migration in China, 1949–2019. China Popul Dev Stud. 3(2):154–159.
Geng H, Shi D, Zhang W, Huang C. 2016. A prediction scheme for the frequency of summer tropical cyclone landfalling over China based on data mining methods. Met Apps. 23(4):587–593.
Grinsted A, Moore JC, Jevrejeva S. 2013. Projected Atlantic hurricane surge threat from rising temperatures. Proc Natl Acad Sci U S A. 110(14):5369–5373.
Haigh ID, Wadey MP, Wahl T, Ozsoy O, Nicholls RJ, Brown JM, Horsburgh K, Gouldby B. 2016. Spatial and temporal analysis of extreme sea level and storm surge events around the coastline of the UK. Sci Data. 3(1):160107.
Hallegatte S, Green C, Nicholls RJ, Corfee-Morlot J. 2013. Future flood losses in major coastal cities. Nature Clim Change. 3(9):802–806.
Helderop E, Grubesic TH. 2019. Social, geomorphic, and climatic factors driving U.S. coastal city vulnerability to storm surge flooding. Ocean Coastal Manag. 181:104902.
Hou JM, Yu FJ, Yuan Y, Fu X. 2011. [Spatial and temporal distribution of red tropical storm surge disasters in China]. Marine Sci Bull. 30(5):535–539. (Chinese).
Huang D. 2018. Research of tracks clustering and the variation of cold wave based on FMM algorithm [dissertation]. Nanjing: Nanjing University of Information Science & Technology. (Chinese).
Kim H-S, Kim J-H, Ho C-H, Chu P-S. 2011. Pattern classification of typhoon tracks using the fuzzy c-means clustering method. J Climate. 24(2):488–508.
Kim H-K, Seo K-H. 2016. Cluster analysis of tropical cyclone tracks over the western north pacific using a self-organizing map. J Climate. 29(10):3731–3751.

Knutson TR, McBride JL, Chan J, Emanuel K, Holland G, Landsea C, Held I, Kossin JP, Srivastava AK, Sugi M. 2010. Tropical cyclones and climate change. Nature Geosci. 3(3): 157–163.

Kovordányi R, Roy C. 2009. Cyclone track forecasting based on satellite images using artificial neural networks. ISPRS J Photogramm Remote Sens. 64(6):513–521.

Ling Z, Wang G, Wang C, Fan Z-S. 2011. Different effects of tropical cyclones generated in the South China Sea and the northwest Pacific on the summer South China Sea circulation. J Oceanogr. 67(3):347–355.

Liu Y, Chen X, Zhao H, Zhao Q, Zhang D, Fei S. 2018. A method of rapid classification of tropical cyclone tracks over China and its application. J Tropical Meteorol. 24(2):131–141.

Lixin Y, Lingling G, Dong Z, Junxue Z, Zhanwu G. 2012. An analysis on disasters management system in China. Nat Hazards. 60(2):295–309.

Lloyd SJ, Kovats RS, Chalabi Z, Brown S, Nicholls RJ. 2016. Modelling the influences of climate change-associated sea-level rise and socioeconomic development on future storm surge mortality. Clim Change. 134(3):441–455.

Lu X, Yu H, Ying M, Zhao B, Zhang S, Lin L, Bai L, Wan R. 2021. Western north pacific tropical cyclone database created by the China meteorological administration. Adv Atmos Sci. 38(4):690–699..

Luo S, Cai F, Liu H, Lei G, Qi H, Su X. 2015. Adaptive measures adopted for risk reduction of coastal erosion in the People's Republic of China. Ocean Coastal Manag. 103:134–145.

Ma Z, Melville DS, Liu J, Chen Y, Yang H, Ren W, Zhang Z, Piersma T, Li B. 2014. Rethinking China's new great wall. Science. 346(6212):912–914.

Mcivor A, Spencer T, Möller I, Spalding M. 2012. Storm surge reduction by mangroves. [accessed 2020 Jul 15]. http://www.mangrovealliance.org/wp-content/uploads/2018/05/storm-surge-reduction-by-mangroves-1.pdf.

Meng Y, Lu J, Liao QL. 2005. Analysis of characteristics of the West-Pacific typhoon affecting the sea area around the island of Taiwan. J Trop Meteorol. (03):315–332. (Chinese). https://kns.cnki.net/kcms/detail/detail.aspx?dbcode=CJFD&dbname=CJFD2005&filename=RDQX200503011&uniplatform=NZKPT&v=t9a2YbNlCb%25mmd2BCCO6GL7QCeSOWBJiJU7OUbPZgMOI6buHu6fyjDGHDK4JVLHjZDjQx

MNRC Ministry of Natural Resources of the People's Republic of China. 2019. Bulletin of China Sea Level. 2018. Accessed 2020 July 15. http://gi.mnr.gov.cn/201905/t20190510_2411195.html

National Bureau of Statistics. 2019. China Statistical Yearbook. Beijing: China Statistics Press.

Nakamura J, Lall U, Kushnir Y, Camargo SJ. 2009. Classifying north Atlantic tropical cyclone tracks by mass moments. J Climate. 22(20):5481–5494.

Needham HF, Keim BD, Sathiaraj D, Shafer M. 2013. A global database of tropical storm surges. Eos Trans Agu. 94(24):213–214.

Neumann B, Vafeidis AT, Zimmermann J, Nicholls RJ. 2015. Future coastal population growth and exposure to sea-level rise and coastal flooding-a global assessment. PLoS One. 10(3): e0118571.

Oceanic Administration of Guangxi. 2008–2009. Bulletin of Guangxi marine ecological environment status.

Overpeck JT, Otto-Bliesner BL, Miller GH, Muhs DR, Alley RB, Kiehl JT. 2006. Paleoclimatic evidence for future ice-sheet instability and rapid sea-level rise. Science. 311(5768): 1747–1750.

Rahmstorf S. 2007. A semi-empirical approach to projecting future sea-level rise. Science. 315(5810):368–370.

Ramsay HA, Camargo SJ, Kim D. 2012. Cluster analysis of tropical cyclone tracks in the Southern Hemisphere. Clim Dyn. 39(3-4):897–917.

Resio DT, Westerink JJ. 2008. Modeling the physics of storm surges. Phys Today. 61(9):33–38.

Rodrigo SMT, Villanoy CL, Briones JC, Bilgera PHT, Cabrera OC, Narisma GTT. 2018. The mapping of storm surge-prone areas and characterizing surge-producing cyclones in Leyte Gulf. Nat Hazards. 92(3):1305–1320.

Roy C, Kovordányi R. 2012. Tropical cyclone track forecasting techniques - a review. Atmos Res. 104-105:40–69.
Shi X, Liu S, Yang S, Liu Q, Tan J, Guo Z. 2015. Spatial-temporal distribution of storm surge damage in the coastal areas of China. Nat Hazards. 79(1):237–247.
Spalding MD, McIvor AL, Beck MW, Koch EW, Möller I, Reed DJ, Rubinoff P, Spencer T, Tolhurst TJ, Wamsley TV, et al. 2014. Coastal ecosystems: a critical element of risk reduction. Conservation Lett. 7(3):293–301.
State Oceanic Administration of China. 2017. Bulletin of China marine disaster. [accessed 2020 Jul 15]. http://www.mnr.gov.cn/sj/sjfw/hy/gbgg/zghyzhgb/.
State Oceanic Administration of China. 1989–2018. Bulletin of China marine disaster. [accessed 2020 Jul 15]. http://www.mnr.gov.cn/sj/sjfw/hy/gbgg/zghyzhgb/.
STI (Shanghai Typhoon Institute). 2020. Best track dataset. [accessed 2020 Jul 15]. http://tcdata.typhoon.org.cn/zjljsjj_zlhq.html.
Sun J, Zuo CJ, Huang L, Cai XJ, Qing Li Q. 2013. Characteristics and causes of typhoon and storm surge along coast of East China Sea. J Hohai Univ Nat Scie. 41(5):461–465. (Chinese).
Wang Y, Liu J, Du X, Liu Q, Liu X. 2021. Temporal-spatial characteristics of storm surges and rough seas in coastal areas of Mainland China from 2000 to 2019. Nat Hazards. 107(2):1273–1285.
Wang K, Yang Y, Reniers G, Huang Q. 2021. A study into the spatiotemporal distribution of typhoon storm surge disasters in China. Nat Hazards. 108(1):1237–1256.
Wang BF, Zhai QF, Ao X, Zhao YJ, Ren ZY, Zhu DH, Liu NN, Qi C, Zhao XQ. 2014. Analysis of storm surge disasters in Liaoning. J Anhui Agric Sci. 42(6):1765–1768. (Chinese).
Winther JG, Dai M, Rist T, Hoel AH, Li Y, Trice A, Morrissey K, Juinio-Meñez MA, Fernandes L, Unger S, et al. 2020. Integrated ocean management for a sustainable ocean economy. Nat Ecol Evol. 4(11):1451–1458.
Yasuda T, Nakajo S, Kim SY, Mase H, Mori N, Horsburgh K. 2014. Evaluation of future storm surge risk in East Asia based on state-of-the-art climate change projection. Coastal Eng. 83:65–71.
Ying M, Zhang W, Yu H, Lu XQ, Feng JX, Fan Y, Zhu YT, Chen DQ. 2014. An overview of the china meteorological administration tropical cyclone database. J Atmos Oceanic Technol. 31(2):287–301.
Yu FJ, Dong JX, Ye L. 2015. Collection of storm surge disasters historical data in China 1949–2009. Beijing: China Ocean Press.
Zeng R. 2018. Construction of the monitoring, prevention and control system for marine hazards: a case study of the Lianjiang comprehensive demonstration zone against marine disaster. Ocean Dev Manag. 35(02):74–77. (Chinese).
Zhang X, Yi L, Zhao D. 2013. Community-based disaster management: a review of progress in China. Nat Hazards. 65(3):2215–2239.